frontiers in Soil Science

TYPE Original Research
PUBLISHED 12 February 2026
DOI 10.3389/fsoil.2026.1746654

OPEN ACCESS

EDITED BY
Anna De Marco,
University of Naples Federico II, Italy

REVIEWED BY
Paurabi Das,
Council of Scientific and Industrial Research (CSIR), India
Mohamed Ali Borgi,
University of Gafsa, Tunisia

*CORRESPONDENCE
Henry Díaz-Chuquizuta
henry.diazchuquizuta@unas.edu.pe

RECEIVED 14 November 2025
REVISED 31 December 2025
ACCEPTED 26 January 2026
PUBLISHED 12 February 2026

CITATION
Díaz-Chuquizuta H, Malca Quezada ME, Vallejos-Torres G, Cuevas-Giménez JP, Huamaní Yupanqui HA, Sánchez Ojanasta M, Solórzano R and Martínez B (2026) Antagonistic interaction between zinc and cadmium in cocoa (*Theobroma cacao* L. var. CCN-51) seedlings amended with rock phosphate. *Front. Soil Sci.* 6:1746654. doi: 10.3389/fsoil.2026.1746654

Antagonistic interaction between zinc and cadmium in cocoa (*Theobroma cacao* L. var. CCN-51) seedlings amended with rock phosphate

Henry Díaz-Chuquizuta [1]*, María Esmilda Malca Quezada [2], Geomar Vallejos-Torres [2], Juan Pablo Cuevas-Giménez [3], Hugo Alfredo Huamaní Yupanqui [4], Martín Sánchez Ojanasta [2], Richard Solórzano [5] and Boris Martínez [1]

[1]Estación Experimental Agraria San Ramón. Dirección de Desarrollo Tecnológico Agrario, Instituto Nacional de Innovación Agraria (INIA), Yurimaguas, Alto Amazonas, Peru, [2]Dirección de Servicios Estratégicos Agrarios, Estación Experimental Agraria El Porvenir, Instituto Nacional de Innovación Agraria (INIA), Juan Guerra, San Martín, Peru, [3]Dirección de Servicios Estratégicos Agrarios, Estación Experimental Agraria de Baños del Inca, Instituto Nacional de Innovación Agraria (INIA), Cajamarca, Peru, [4]Docente Investigador de la Universidad Nacional Agraria de la Selva, Tingo María, Peru, [5]Dirección de Servicios Estratégicos Agrarios, Instituto Nacional de Innovación Agraria (INIA), Lima, Peru

Introduction: In the San Martın region, several studies have reported Cd concentrations in surface soils approaching the upper limit (UL), with mean values ranging from 0.27 to 1.351 mg·kg^{-1}.

Methods: Cadmium (Cd) transfer to *Theobroma cacao* (CCN-51) seedlings was evaluated under 12 factorial combinations of phosphate rock (RFP) and foliar zinc sulphate ($ZnSO_4$) applications, using relative uptake (foliar Cd/soil Cd) as the primary response variable.

Results: The treatment showing the highest Cd uptake was T4, defined as RFP = 0 mg·kg^{-1} and $ZnSO_4$ = 527.80 mg·plant-1, with a value of 53.12. The observed range in relative uptake was 33.08 units, indicating substantial variation among management combinations. At the factor-level analysis, the high RFP treatment (114.55 mg·kg^{-1}) was associated with an average reduction of approximately 26.5% in relative uptake and lower within-group variability compared to the 0 mg·kg^{-1} level. Interaction plots indicated that the effect of $ZnSO_4$ on nutrient uptake depended on RFP level, with a descending response profile at high RFP concentrations. In parallel, soil correlation analyses identified available phosphorus and pH as the principal modulators of Cd transfer from soil to plant. Leaf-level principal component analysis showed that Zn and K were projected in the opposite direction to P_2O_5 and Cd, consistent with an ionic balance mechanism regulating Cd accumulation, and achieved an overall classification accuracy of approximately 81%, thereby confirming multivariate separability among treatments.

Discussion: Collectively, these integrated results support identifying T4 as the treatment with the highest Cd uptake within the evaluated set. Accordingly, the presence of Zn^{2+}–Cd^{2+} antagonism can be asserted; however, its expression is strongly influenced by soil pH and, most critically, by the availability of phosphorus derived from RFP.

KEYWORDS
cadmium, cocoa, LDA, PCA, phosphate rock, relative uptake, zinc

1 Introduction

Cocoa (*Theobroma cacao* L.) underpins global value chains and rural livelihoods. During the 2023/24 season, the global market experienced a supply deficit, with production reaching approximately 4.38 million tonnes compared to 4.82 million tonnes of grindings, underscoring its economic significance and the need to ensure product quality and safety (1). Geographically, Latin America and the Caribbean account for approximately 20% of global cocoa production, led by Ecuador, Brazil, Peru, the Dominican Republic, and Colombia, where smallholder producers are predominant (2). These production dynamics coexist with increasingly stringent regulations on cadmium (Cd^{2+}) concentrations in cocoa and chocolate within the European Union (EU), which affect market access and highlight the urgent need for implementing effective agronomic mitigation strategies (3).

In Peru, cocoa holds strategic importance in both production volume and its positioning in the fine aroma category. In 2023, national production reached 163,300 tonnes, led by San Martín (62,200 tonnes; 38.1% share), followed by Junín, Ucayali, Huánuco, and Cusco (4). Regarding land use, the national harvested area was 198,145 ha in 2023 and 187,113 ha in 2024, with an average national yield of 835 $kg{\cdot}ha^{-1}$ in 2024 (5). Spatial heterogeneity of Cd^{2+} concentrations in soils and grains across the country has been documented: elevated levels are primarily confined to the northern regions (Amazonas, Loreto, Tumbes, Piura) and to localized areas in the central zone (Huánuco, San Martín), with soil Cd^{2+} identified as the dominant predictor of grain Cd^{2+} content (6).

At the regional level, San Martín is the leading cocoa-producing area in Peru. In 2022, it reported 65,011.7 ha under cultivation and 64,680.8 tonnes of production, with reference yields closer to 731 $kg{\cdot}ha^{-1}$ among producer organizations (SIEA-MIDAGRI, cited in 7). The region maintained its leadership in 2023, producing 62.2 thousand tonnes (4). In Loreto, the harvested area increased from 891 ha in 2023 to 912 ha in 2024, while production rose from 1,257 t to 1,373 t, respectively, corresponding to a yield of 1,506 $kg{\cdot}ha^{-1}$ in 2024, indicating recent improvements in productivity (5). At the broader Latin American level, national Cd^{2+} mapping efforts in Colombia have strengthened soil management strategies and regulatory compliance, aligning with EU requirements (8), and providing a relevant framework for the Peruvian context. Similarly, in the San Martín region, several studies have reported Cd concentrations in surface soils approaching the upper limit (UL), with mean values ranging from 0.27 to 1.351 $mg{\cdot}kg^{-1}$ (9). In contrast, Luis-Alaya et al. (10) reported soil Cd concentrations of 1.09 $mg{\cdot}kg^{-1}$, which are below the tolerable limit for agricultural soils (≥ 1.4 $mg{\cdot}kg^{-1}$). Although the UL for soil Cd was not exceeded, elevated Cd concentrations were observed in the roots, leaves, and grains of CCN-51 cocoa, with mean values of 1.87, 2.06, and 1.12 $mg{\cdot}kg^{-1}$, respectively (11).

From a mechanistic perspective, zinc (Zn^{2+}) can antagonize the absorption and translocation of Cd^{2+} through competition for transporters and the regulation of uptake pathways; however, its effectiveness is context-dependent, influenced by factors such as pH, available phosphorus, Ca^{2+} concentration, mineralogy, and soil microbiota, and typically operates within specific dosage ranges. Phosphate sources (e.g., phosphate rock) promote the immobilization or passivation of Cd^{2+} in soils through precipitation and adsorption processes, thereby modulating its bioavailability to plants (2, 3, 6, 8).

This study aims to assess the antagonistic interaction between zinc sulphate ($ZnSO_4$) and cadmium (Cd^{2+}) in cocoa (*Theobroma cacao* var. CCN-51) seedlings under phosphate rock amendment, using integrated soil–leaf–biometric analyses to identify the treatment with the lowest relative Cd^{2+} uptake.

2 Materials and methods

2.1 Study area (location and climate)

The study was conducted at the San Ramón Agrarian Experimental Station of the National Institute of Agrarian Innovation (INIA), located in the Yurimaguas district, Alto Amazonas province, Loreto region, Peru (approximately 5.90° S, 76.12° W). Yurimaguas has a humid tropical climate typical of the lower Amazon, with average monthly temperatures of approximately 26–27 °C (temperature normals reported for Yurimaguas) and annual precipitation ranging from ~2,500 to 2,600 mm, characterized by pronounced seasonal rainfall. Intra-annual temperature variation is minimal, and rainfall is persistent throughout the year. Winds are generally weak (around 1–2 $m{\cdot}s^{-1}$), and relative humidity remains high year-round (> 70%). These climatic conditions have been documented for Yurimaguas and the Huallaga basin in both international and regional climate sources, including compilations of local monthly climate normals (12).

2.2 Plant material, substrate, and greenhouse management

Cocoa (*Theobroma cacao* L.) seedlings of the CCN-51 clone were used, established in a greenhouse, and evaluated up to four months of age. The seedlings were grown in 2 kg polyethylene bags filled with a local agricultural substrate (one plant per bag). The soil used in the trial was pre-incubated for 45 days after amendment-conditioning with phosphorus sources (phosphate rock) and prior to transplanting to stabilize the soil–amendment reactions. Foliar application of zinc sulphate began once the seedlings developed true leaves, with four applications administered at 15-day intervals using a manual backpack sprayer with a fine-cone nozzle to ensure uniform foliage coverage. Biometric evaluations (plant height, stem diameter, number of leaves, root length, and root volume) were conducted every 30 days during the four-month greenhouse period.

2.3 Experimental design and treatments

The preliminary soil characteristics prior to treatment application were as follows: 5.29 pH, 1.61% organic matter content (OM), 0.07% total nitrogen (N), 6.95 $mg{\cdot}kg^{-1}$ available phosphorus (P); 75.97 $mg{\cdot}kg^{-1}$ available potassium (K), 0.06 $mg{\cdot}kg^{-1}$ available cadmium (Cd), 0.25 $mg{\cdot}kg^{-1}$ total cadmium, and a sandy

10.3389/fsoil.2026.1746654

loam texture. A 3 × 4 factorial arrangement was implemented in a completely randomized design, with three replicates per factor combination, resulting in 36 experimental units. The results of each treatment are seen in Table 1. The selection of rock phosphate (RFP) and zinc sulfate ($ZnSO_4$) levels was based on agronomic, edaphic, and mechanistic considerations. The RFP rates (0, 57.27, and 114.55 mg·kg^{-1}) represent a gradient from zero phosphorus input to a high application dose, designed to evaluate the potential of RFP to modify soil pH, increase phosphorus availability, and promote Cd immobilization through the formation of Cd–phosphate complexes, while also accounting for the possible presence of Cd impurities in natural phosphate sources. The $ZnSO_4$ doses (0, 98.80, 197.50, and 527.80 mg·plant^{-1}, applied foliarly) were defined based on reported ranges effective in inducing Zn–Cd physiological antagonism without causing phytotoxic effects. This approach enabled the assessment of dose-dependent responses and interactions with soil phosphorus. Consequently, the factorial experimental design facilitates the identification of management combinations with the greatest potential to mitigate Cd transfer from soil to plant.

2.4 Variables measured and sampling procedures

The operational database was structured into three measurement compartments: soil, leaf tissue, and seedling, each containing representative variables. Soil variables included pH, organic matter (OM, %), total nitrogen (N, %), available phosphorus (P_2O_5, mg·kg^{-1}), available potassium (K_2O, mg·kg^{-1}), exchangeable cations (Ca^{2+}, Mg^{2+}, K^+, Na^+), effective cation exchange capacity (ECEC), and trace metals (available Cd^{2+}, Zn^{2+}, and Cu^{2+}). Leaf tissue variables comprised macronutrients (P_2O_5, K_2O, Ca^{2+}, Mg^{2+}, Na^+) and micronutrients (Fe^{3+}, Mn^{2+}, Cu^{2+}, Pb^{2+}, Cd^{2+}, Zn^{2+}), expressed in ppm or percentage depending on analytical practice. Seedling variables included substrate pH, plant height (cm), stem diameter (mm), number of leaves, root length (cm), and root volume (mL). Analytical determinations followed INIA's standard laboratory protocols: pH was measured by potentiometry, macronutrients by extraction and colorimetry or flame photometry depending on the measured analyte, and metals by acid digestion with detection by Atomic Absorption Spectroscopy (AAS) or Inductively Coupled Plasma–Optical Emission Spectrometry (ICP–OES). Treatment coding and sample traceability were maintained following the field logbook and experimental data matrix.

2.5 Statistical analysis

All analyses were conducted in R version 4.x using RStudio/Posit IDE, with fully reproducible scripts in R Markdown or Quarto. The analytical workflow relied on the tidyverse, ggplot2, rstatix, corrplot, FactoMineR/factoextra, MASS, and car packages (13–15).

Descriptive statistics and exploratory data analysis (EDA) included means, standard deviations (SD), 95% confidence intervals (95%CI), coefficients of variation (CV), skewness, and kurtosis to characterize soil, leaf, and seedling variables and verify assumptions before modelling (15, 16). Correlation analyses and heatmaps were used to examine Pearson correlation matrices and visualise covariation (e.g., P_2O_5–Cd^{2+}, K_2O–Zn^{2+}) and detect collinearity before multivariate analysis (17). This study reported high correlations within each compartment. Principal Component Analysis (PCA) was applied separately to soil, leaf, and seedling datasets using prcomp and FactoMineR to reduce dimensionality, synthesise latent axes (e.g., P_2O_5–(Cd^{2+}, Zn^{2+})–K_2O vs pH/Na^+), and visualise gradients (18, 19). The study details the variance explained by the first two components. Factorial ANOVA/GLM ($ZnSO_4$ × RFP) was used to assess main and interaction effects, with verification for assumptions and effect sizes (20). A pattern of non-parallel lines in the interaction plots supports a $ZnSO_4$ × RFP interaction (Table 1). Visual moderation analysis (scatterplots and simple slopes), using dispersion plots by RFP level and simple slope analysis, helps to interpret the direction and magnitude of the interaction (21), where slopes are expected to decrease with higher RFP levels.

Boxplots were used to compare medians, interquartile ranges (IQRs), and outliers robustly among RFP × $ZnSO_4$ treatments (22), showing clear separations between treatment combinations. Linear Discriminant Analysis (LDA) was applied as a supervised classification method to evaluate treatment separability based on seedling traits, complementing PCA (18). Finally, the relative uptake index (foliar Cd^{2+}/soil Cd^{2+}) was used as a dimensionless metric to prioritize treatments with lower soil-to-plant transfer efficiency, providing evidence of attenuation under high RFP levels (6, 23).

Prior to multivariate analyses (PCA and LDA), all variables were centered and scaled using z-score standardization, resulting in

TABLE 1 Description of the experimental treatments.

Treatments	Phosphoric rock - RFP (g)	Zinc sulphate - ZnSO4 (mg)	Combinations
T1	0	0	0
T2		98.8	98.8 ZnSO4
T3		197.5	197.5 ZnSO4
T4		527.8	527.8 ZnSO4
T5	52.27	0	52.27 RFP
T6		98.8	52.27 RFP + 98.8 ZnSO4
T7		197.5	52.27 RFP + 197.5 ZnSO4
T8		527.8	52.27 RFP + 527.8 ZnSO4
T9	114.55	0	114.55 REP
T10		98.8	114.55 RFP + 98.8 ZnSO4
T11		197.5	114.55 RFP + 197.5 ZnSO4
T12		527.8	114.55 RFP + 527.8 ZnSO4

a mean of zero and a unit variance for each variable. This transformation was required to account for differences in units and magnitudes among variables (e.g., pH, mg·kg^{-1}, cmol(+)·kg^{-1}, and biometric traits), ensuring that no variable artificially dominated the multivariate structure. No additional logarithmic transformations were applied, as preliminary exploratory analyses did not indicate extreme deviations or skewness that would justify their use.

3 Results

3.1 Descriptive statistics

Overall, the soil exhibited low to moderate acidity (pH: M = 5.52, SD = 0.61, 95% CI [5.32, 5.72]; n = 36), with a right-skewed distribution (skew = 1.01) and mesokurtic kurtosis of 0.25. The pronounced dispersion of Cd^{2+} and P indicates heterogeneous soil nutrient supply, which may influence foliar Cd^{2+} uptake and modulate the plant's response to $ZnSO_4$ (Table 2). Foliar Zn^{2+} levels were elevated, with moderate dispersion (M = 78.49 mg·kg^{-1}, SD = 25.65, 95% CI [69.86, 87.11], CV = 32.7%). Regarding the Zn^{2+}–Cd^{2+} ratio, the average foliar Zn^{2+}: Cd^{2+} ratio was approximately 7.1:1. This ratio suggests a favourable relative availability of Zn^{2+} despite the high and heterogeneous foliar Cd^{2+} concentrations. Nonetheless, descriptive statistics alone do not demonstrate Zn–Cd antagonism; rather, they contextualize the magnitude and variability on which the treatments operate (Table 3). Seedling biometrics showed that the aerial traits were stable to moderately variable: seedling height (M = 22.76 cm, SD = 3.81, 95% CI [21.47, 24.05], CV = 16.8%) and stem diameter (M = 7.92 mm, SD = 0.79, 95% CI [7.66, 8.17], CV = 10.1%). This pattern indicates that that the greater dispersion observed in root traits suggests that management factors ($ZnSO_4$ and phosphate rock) and/or the availability of Cd^{2+} and P (PO_4^{3-}) in the soil exert a more substantial influence on root architecture than on aerial biomass at this stage.

3.2 Correlation analysis and heatmap visualization

The correlations based on soil analysis results revealed a strong covariation block among available phosphorus (P_2O_5; as PO_4^{3-} in solution), total cadmium (Cd^{2+}), exchangeable cations, and pH. Extremely high correlations were observed between P_2O_5 and exchangeable K^+ (cmol(+)·kg^{-1}; (r(34) = 0.97, p < 0.001), P_2O_5 and exchangeable Na^+ (cmol(+) ·kg^{-1}; r(34) = 0.95, p < 0.001), as well as between P_2O_5 and Cd^{2+} (r(34) = 0.93, p < 0.001). Cadmium also correlated strongly with K^+ (r(34) = 0.92, p < 0.001) and Na^+ (r(34) = 0.90, p < 0.001). Soil pH was positively correlated with P_2O_5, Cd^{2+}, K^+, and Na^+ (r ≈ 0.73–0.75, p < 0.001), and moderately with soil Zn^{2+} (r = 0.45, p < 0.01). In contrast, K_2O (mg·kg^{-1}) showed weak or non-significant relationships with most variables (|r| ≤ 0.27, ns). These correlations suggest that phosphate rock (RFP) applications simultaneously increased soil P_2O_5 (PO_4^{3-}), pH, and exchangeable cations (K^+, Na^+), while soil Cd^{2+} co-increased with these factors, likely due to cadmium impurities in the RFP and/or co-accumulation in the extracted fractions. The positive pH–Cd^{2+} correlation (rather than the expected negative relationship) supports the hypothesis of a shared source of Cd rather than changes in availability driven by soil chemistry (Figure 1).

Correlations based on leaf concentration data revealed strong covariation between nutrients and cadmium. Very high correlations were observed for P_2O_5–Cd^{2+} (r(34) = 0.88, p < 0.001) and Na^+–Cd^{2+} (r(34) = 0.84, p < 0.001). High correlations were also found for

TABLE 2 Descriptive analysis of soil physicochemical properties after the application of different RFP doses.

Variable	Vars	N	Mean	Sd	Median	Min	Max	Range	Skew	Kurtosis	Se
pH	1	36	5.52	0.61	5.6	4.48	7.85	3.37	1.01	4.15	0.1
P_2O_5 (mg·kg^{-1})	2	36	49.38	35.26	65.56	3.98	95.27	91.28	-0.22	-1.68	5.88
K_2O (mg·kg^{-1})	3	36	116.42	50.68	101.83	52.73	269.33	216.61	1.3	1.35	8.45
Zn^{2+} (mg·kg^{-1})	4	36	10.3	4.15	9.72	5.84	24.2	18.36	1.75	3.09	0.69
Cd^{2+} (mg·kg^{-1})	5	36	0.4	0.31	0.41	0.01	0.96	0.94	0.11	-1.38	0.05
K^+ (cmol(+)·kg^{-1})	6	36	0.18	0.14	0.2	0	0.42	0.42	-0.08	-1.48	0.02
Na^+ (cmol(+)·kg^{-1})	7	36	1.5	1.1	2.01	0	2.75	2.75	-0.53	-1.59	0.18

TABLE 3 Descriptive analysis of foliar nutrient contents in 4-month-old cocoa seedlings.

Variable	Vars	N	Mean	Sd	Median	Min	Max	Range	Skew	Kurtosis	Se
P_2O_5 (mg·kg^{-1})	1	36	4887.41	2401.38	5314.85	1154.87	9903.13	8748.26	0.11	-1.13	400.23
K_2O (mg·kg^{-1})	2	36	14575.1	3682.25	14320	7606.25	22276.7	14670.4	0.37	-0.62	613.71
Zn^{2+} (mg·kg^{-1})	3	36	78.15	25.57	77.12	33.26	137.83	104.57	0.59	0.09	4.26
Cd^{2+} (mg·kg^{-1})	4	36	10.95	7.94	12.99	0.89	26.41	25.52	-0.06	-1.35	1.32
Na^+ (cmol(+)·kg^{-1})	5	36	24293.2	20102.5	17309.1	2862.21	61614	58751.7	0.55	-1.29	3350.41

10.3389/fsoil.2026.1746654

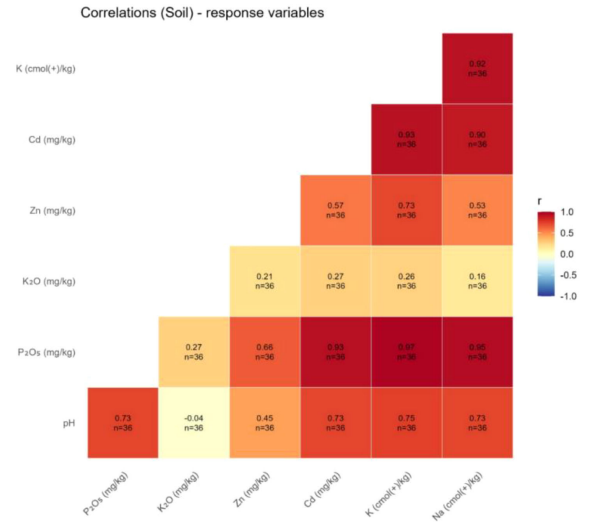

FIGURE 1
Soil correlation matrix and heatmap showing relationships among chemical variables.

K_2O–Zn^{2+} (r(34) = 0.72, p < 0.001), P_2O_5–Na^+ (r(34) = 0.77, p < 0.001), and P_2O_5–Zn^{2+} (r(34) = 0.64, p < 0.001). The Zn^{2+}–Cd^{2+} association was moderate to high (r(34) = 0.59, p < 0.001), and K_2O–Cd^{2+} showed a moderate correlation (r(34) = 0.37, p < 0.05). Only K_2O–Na^+ was not significant (r = 0.12, ns). These results indicate that, in strictly correlational terms, foliar Zn^{2+} is positively associated with Cd^{2+} (r = 0.59). This pattern does not support a simple antagonistic relationship at the leaf level. Instead, it suggests treatment collinearity (e.g., higher $ZnSO_4$ doses applied alongside greater RFP inputs) or shared uptake drivers, such as increased plant vigour or co-transport under elevated P_2O_5 and Na^+ supply (Figure 2).

In the biometric correlations of 4-month-old cocoa seedlings, strong and consistent associations were observed among growth traits. Seedling height and root length showed a very strong correlation (r(34) = 0.88, p < 0.001), indicating that taller seedlings also tend to develop longer roots. Seedling height and stem diameter were moderately to highly correlated (r(34) = 0.58, p < 0.001), and stem diameter and root length exhibited a similar moderate-high association (r(34) = 0.57, p < 0.001). Together, these three relationships suggest a coordinated growth pattern between aerial and root structures, supporting the notion that treatments enhance overall vigour (e.g., combinations of RFP and $ZnSO_4$) promote simultaneous aerial and root development (Figure 3).

Other associations were weak or non-significant: number of leaves with seedling height (r = 0.30, ns) and with root length (r = 0.22, ns). Root volume was also unrelated to the remaining traits (|r| ≤ 0.08, ns). This suggests that root volume was either more variable or less effectively captured by the experimental arrangement compared with root length and seedling diameter.

3.3 Principal component analysis

The PCA of the soil analysis results explained 85.4% of the total variance (Dim1 = 70.5%; Dim2 = 14.9%; Table 4; Figure 4). Dim1 grouped the fertility/chemical status variables, dominated by pH, P_2O_5, Zn^{2+}, Cd^{2+}, K^+ (cmol(+)·kg^{-1}), and Na^+ (cmol(+)·kg^{-1}), as shown in Table 5. The small angles between these vectors, all oriented toward the positive semi-axis of Dim1 in Figure 4, indicate strong positive correlations within this block, consistent with the patterns observed in the heat maps. Dim2 was clearly dominated by K_2O (the longest vector and the most significant contributor), showing that variability in soil K represents an independent component separate from the main pH–P_2O_5–(Zn^{2+}, Cd^{2+})–exchangeable bases (K^+, Na^+) block (Figure 5).

The PCA of the foliar analyses conducted on 4-month-old cocoa seedlings accounted for 90.0% of the total variance across the first two dimensions (Dim1 = 67.6%; Dim2 = 22.4%; Table 6, Figure 6). Dim1 represents a clear ion-accumulation axis: K_2O and Zn^{2+} exhibited the most significant contributions (longest vectors and highest chromatic intensity), followed by Na^+, whereas Cd^{2+}

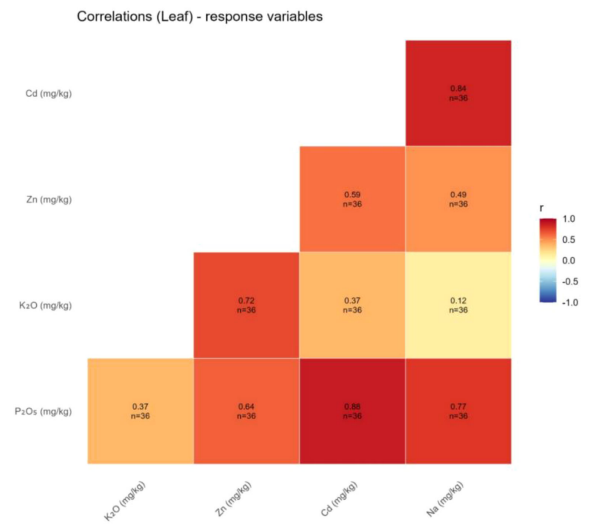

FIGURE 2
Correlation matrix and heatmap showing relationships among foliar nutrient concentrations.

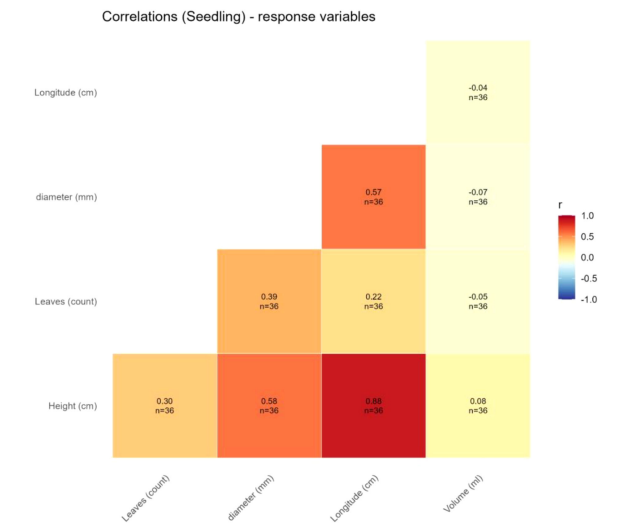

FIGURE 3
Correlation matrix and heatmap showing relationships among seedling biometric traits.

10.3389/fsoil.2026.1746654

TABLE 4 Summary of boxplots by treatment.

Treatment	Variable	n	Mean	Sd	Min	Max
T1	Seedling height (cm)	3	30.167	2.581	27.2	31.9
T1	Stem diameter (mm)	3	4.56	0.426	4.07	4.84
T1	Number of leaves	3	10	1	9	11
T1	Root length (cm)	3	31.667	1.756	30	33.5
T1	Root volume (mL)	3	1.333	0.577	1	2
T10	Seedling height (cm)	3	24.533	1.102	23.8	25.8
T10	Stem diameter (mm)	3	3.847	0.126	3.73	3.98
T10	Number of leaves	3	11	4.583	6	15
T10	Root length (cm)	3	17	1.323	15.5	18
T10	Root volume (mL)	3	2.667	0.577	2	3
T11	Seedling height (cm)	3	21.433	2.409	19.8	24.2
T11	Stem diameter (mm)	3	3.88	0.214	3.71	4.12
T11	Number of leaves	3	8	1.732	7	10
T11	Root length (cm)	3	8	2.646	6	11
T11	Root volume (mL)	3	2.167	0.764	1.5	3
T12	Seedling height (cm)	3	21.3	1.3	19.8	22.1
T12	Stem diameter (mm)	3	3.927	0.085	3.84	4.01
T12	Number of leaves	3	9.667	2.082	8	12
T12	Root length (cm)	3	8.5	0.5	8	9
T12	Root volume (mL)	3	1.967	0.153	1.8	2.1
T2	Seedling height (cm)	3	34.133	2.401	31.7	36.5
T2	Stem diameter (mm)	3	4.5	0.01	4.49	4.51
T2	Number of leaves	3	11.333	1.528	10	13
T2	Root length (cm)	3	33	4	29	37
T2	Root volume (mL)	3	1.333	0.577	1	2
T3	Seedling height (cm)	3	33.033	0.839	32.5	34
T3	Stem diameter (mm)	3	4.613	0.325	4.28	4.93
T3	Number of leaves	3	10.667	1.528	9	12
T3	Root length (cm)	3	36.833	5.252	31.5	42
T3	Root volume (mL)	3	1.333	0.577	1	2
T4	Seedling height (cm)	3	32.733	2.108	30.4	34.5
T4	Stem diameter (mm)	3	4.69	0.164	4.51	4.83
T4	Number of leaves	3	11	1	10	12
T4	Root lenght (cm)	3	30.2	2.594	27.3	32.3
T4	Root volume (mL)	3	3.333	1.155	2	4
T5	Seedling height (cm)	3	26.333	1.069	25.1	27
T5	Stem diameter (mm)	3	4.72	0.178	4.58	4.92
T5	Number of leaves	3	13.333	0.577	13	14
T5	Root lenght (cm)	3	18.5	1.5	17	20
T5	Root volume (mL)	3	1.667	1.155	1	3
T6	Seedling height (cm)	3	30.667	3.201	27	32.9
T6	Stem diameter (mm)	3	4.717	0.292	4.38	4.9
T6	Number of leaves	3	13.333	1.528	12	15
T6	Root length (cm)	3	24.333	0.764	23.5	25

(Continued)

10.3389/fsoil.2026.1746654

TABLE 4 Continued

Treatment	Variable	n	Mean	Sd	Min	Max
T6	Root volume (mL)	3	1.667	1.155	1	3
T7	Seedling height (cm)	3	28.333	3.002	25.4	31.4
T7	Stem diameter (mm)	3	4.573	0.211	4.35	4.77
T7	Number of leaves	3	11.333	1.155	10	12
T7	Root length (cm)	3	17.367	3.58	15.3	21.5
T7	Root volume (mL)	3	1.833	0.289	1.5	2
T8	Seedling height (cm)	3	27.4	2.666	24.4	29.5
T8	Stem diameter (mm)	3	4.683	0.495	4.18	5.17
T8	Number of leaves	3	13.333	1.528	12	15
T8	Root length (cm)	3	19	4.521	13.8	22
T8	Root volume (mL)	3	2.067	0.902	1.2	3
T9	Seedling height (cm)	3	23.933	1.343	22.4	24.9
T9	Stem diameter (mm)	3	3.803	0.431	3.47	4.29
T9	Number of leaves	3	8	2	6	10
T9	Root length (cm)	3	11.833	1.607	10	13
T9	Root volume (mL)	3	1.5	0.866	1	2.5

and P_2O_5 contributed to a lesser extent (Table 7; Figure 6). Crucially for the Zn^{2+}–Cd^{2+} interaction hypothesis, the Zn^{2+} and Cd^{2+} vectors show opposite orientations along Dim2 (Zn^{2+} with a positive component and Cd^{2+} with a negative component), reflecting an inverse relationship along that axis. This indicates that, at equal levels of the general accumulation axis (Dim1), higher foliar Zn^{2+} levels are associated with lower foliar Cd^{2+} concentrations (Table 7). This pattern is consistent with an antagonistic effect of $ZnSO_4$ on Cd^{2+} uptake or translocation, aligning with the central premise of the study (Figure 6).

The PCA of the biometric analysis results for cocoa seedlings explained 71.6% of the total variance across the first two dimensions (Dim1 = 50.8%; Dim2 = 20.8%), as shown in Figure 4. The vector configuration indicates that Dim1 represents an aerial-size gradient: seedling height and root length load positively and with intermediate magnitude, while stem diameter and number of leaves also align with Dim1, though with smaller contributions (Table 8). The small angles between these vectors in Figure 5 are suggest the positive correlations among them. Dim2 is dominated by root volume, as indicated by the longest vector and highest contribution (Figure 5; Table 8), suggesting that root volume introduces orthogonal variation to aerial size. The biplot shows no distinct separation among the treatment groups (coloured points), suggesting that the RFP × $ZnSO_4$ combinations influence

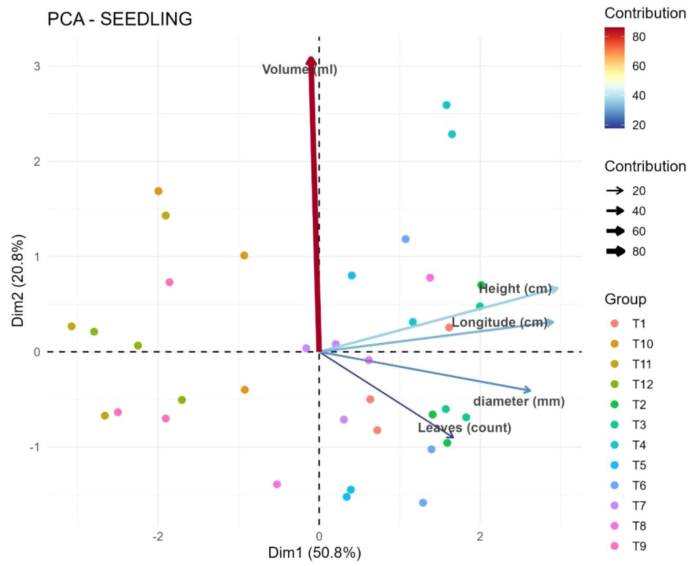

FIGURE 4
Principal component analysis (PCA) of seedling biometric traits.

10.3389/fsoil.2026.1746654

TABLE 5 Relative Cd uptake (foliar Cd/soil Cd).

Treatment	Phosphoric rock dose (RFP, g)	Foliar $ZnSO_4$ dose (mg)	Soil pH	Soil Cd^{+2} ($mg \cdot kg^{-1}$)	Foliar Cd^{+2} ($mg \cdot kg^{-1}$)	Foliar Zn^{2+} ($mg \cdot kg^{-1}$)	Relative uptake
T9	114.55	0	5.86	0.89	17.8	62.72	20.04
T2	0	98.8	5.2	0.04	0.98	67.97	25.43
T1	0	0	5.29	0.04	0.92	35.95	26.11
T12	114.55	527.8	5.81	0.63	16.62	119.76	26.19
T11	114.55	197.5	6.48	0.76	20.42	118.34	26.84
T5	57.27	0	5.53	0.42	11.64	50.19	27.42
T10	114.55	98.8	5.84	0.75	21.41	95.95	28.66
T7	57.27	197.5	5.8	0.39	12.57	76.1	32.22
T8	57.27	527.8	5.63	0.36	11.98	82.28	33.27
T3	0	197.5	4.58	0.03	1.08	75.1	33.73
T6	57.27	98.8	5.6	0.42	14.66	73.62	34.68
T4	0	527.8	4.58	0.02	1.27	79.79	53.12

the magnitude of the traits rather than their covariation pattern. In the context of the study objective, improved morphological performance is associated with positive values along Dim1 (taller seedlings with longer roots) and Dim2 (greater root volume), which may serve as plausible indicators of enhanced tolerance to Cd^{2+} stress when Zn^{2+} supply is adequate.

3.4 Scatter plot analysis and interaction effects

3.4.1 Foliar Zn^{2+}–Cd^{2+} relationship by RFP level

At the treatment level, the covariation between foliar zinc (Zn^{2+}) and foliar cadmium (Cd^{2+}) was positive in the overall analysis (Table 9), indicating that treatments producing higher foliar Zn^{2+} also tended to present higher foliar Cd^{2+}. This trend persisted within each phosphate rock (RFP) level (Figure 7), with positive linear slopes (β) for RFP = 0, 57.27, and 114.55 $mg \cdot kg^{-1}$, as reported in Table 9. Comparatively, the slope magnitude decreased as RFP increased ($\beta_0 > \beta_{57.27} \geq \beta_{114.55}$; Table 3), suggesting attenuation of the Zn^{2+}–Cd^{2+} association at higher RFP levels. These patterns are consistent with a moderating role of RFP. Although RFP does not reverse the direction of the Zn^{2+}–Cd^{2+} relationship within treatments, it weakens its strength, which aligns with an emerging antagonistic component as phosphate availability increases. Overall, the linear correlation between foliar Zn^{2+} and Cd^{2+} was positive at the global level (Table 9) and within each RFP level (Figure 7). The simple slopes (Table 8) were positive across the three RFP levels and decreased in magnitude as the RFP increased, indicating a moderating effect of RFP on the Zn^{2+}–Cd^{2+} relationship.

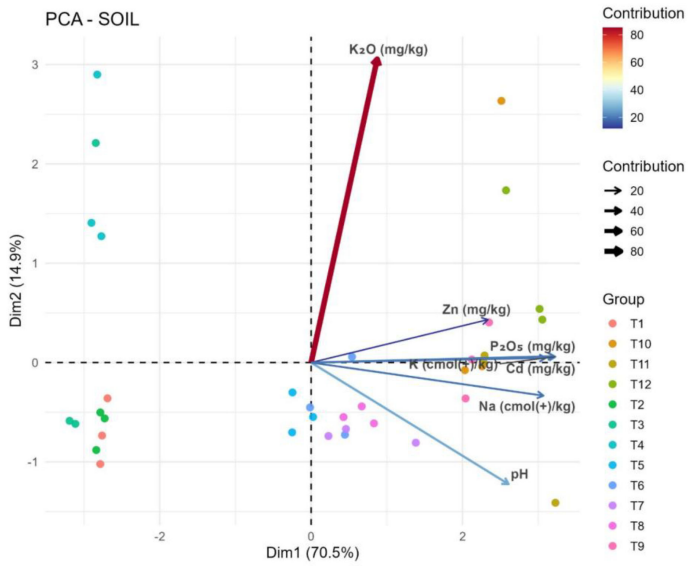

FIGURE 5
Principal component analysis (PCA) of soil variables.

TABLE 6 Regression analysis of the $ZnSO_4$ × RFP interaction on foliar Cd^{2+}.

Term	Estimate	Std.Error	Statistic	P.Value	Conf.Low	Conf.High
(Intercept)	-16.787	12.115	-1.386	0.215	-46.43	12.856
$ZnSO_4$ dose	0.005	0.005	1.005	0.354	-0.007	0.017
Phosphoric rock dose (RFP)	0.352	0.17	2.074	0.083	-0.063	0.767
Soil pH	3.763	2.338	1.609	0.159	-1.959	9.484
Soil Cd^{+2} ($mg{\cdot}kg^{-1}$)	-30.162	24.253	-1.244	0.26	-89.506	29.182
$ZnSO_4$ dose and Phosphoric rock dose (RFP)	0	0	-1.789	0.124	0	0

3.4.2 $ZnSO_4$ × RFP interaction on foliar Cd^{2+}

The line profiles in Figure 8 and the means in Table 10 show that the effect of $ZnSO_4$ dose on foliar Cd^{2+} depends on the RFP level. When RFP = $mg{\cdot}kg^{-1}$, foliar Cd^{2+} increases slightly as $ZnSO_4$ increases. When RFP = 57.27 $mg{\cdot}kg^{-1}$, a non-linear pattern emerges, with an intermediate maximum followed by a slight decrease in foliar Cd^{2+} at higher $ZnSO_4$ doses. When RFP = 114.55 $mg{\cdot}kg^{-1}$, foliar Cd^{2+} exhibits a decreasing trend with increasing $ZnSO_4$. These results indicate that $ZnSO_4$ supplementation does not reduce foliar Cd^{2+} in the absence of RFP; however, when RFP is high, the increase of $ZnSO_4$ levels is associated with lower foliar Cd^{2+} concentrations, consistent with the Zn^{2+}–Cd^{2+} antagonism hypothesis under sufficient phosphate availability. The non-parallel line patterns support the presence of a $ZnSO_4$ × RFP interaction, as also confirmed by Table 11 and Table 6. In summary, the effect of $ZnSO_4$ on foliar Cd^{2+} was moderated by RFP (Figure 8; Table 11). At high RFP (114.55 $mg{\cdot}kg^{-1}$), increasing $ZnSO_4$ corresponded to a reduction in foliar Cd^{2+}, whereas at zero RFP the trend was slightly upward, consistent with a significant $ZnSO_4$ × RFP interaction (Tables 6, 11). In Figure 8, soil Cd refers to the extractable/operationally available fraction, as determined by the extraction method used in the chemical soil analysis, according to INIA laboratory protocols. Given the terminological ambiguity present in the manuscript, references to "total Cd" should be corrected to "available Cd" where appropriate, particularly in analyses addressing soil–plant relationships and foliar Cd uptake.

3.4.3 $ZnSO_4$ × RFP interaction on relative uptake (foliar Cd^{2+}/soil Cd^{2+})

Relative uptake (foliar Cd^{2+}/soil Cd^{2+}) integrates both soil availability and foliar accumulation. In Figure 9, the interaction pattern indicates that when RFP = 0 $mg{\cdot}kg^{-1}$, the relative uptake increases markedly at the highest $ZnSO_4$ dose. At RFP = 57.27 $mg{\cdot}kg^{-1}$, uptake rises at intermediate $ZnSO_4$ doses and then stabilises or slightly declines at the uppermost dose. At the highest RFP level (114.55 $mg{\cdot}kg^{-1}$), relative uptake decreases consistently as $ZnSO_4$ increases. These results indicate that antagonism is clearly expressed under high RFP conditions, where increasing $ZnSO_4$ doses reduce relative uptake, suggesting that Zn^{2+}, in the presence of phosphate, restricts Cd^{2+} transport or bioaccumulation. The interaction effect sizes (partial η^2), reported in Table 12, quantify the practical significance of this phenomenon. In summary, relative Cd^{2+} uptake exhibited a significant $ZnSO_4$ × RFP interaction (Figure 9). At high RFP, relative uptake declined with increasing $ZnSO_4$, supporting a Zn^{2+}–Cd^{2+} antagonistic

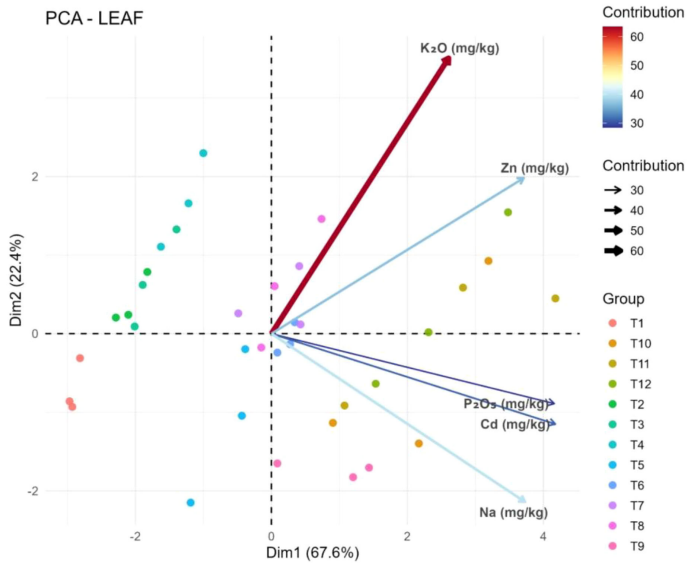

FIGURE 6
Principal component analysis (PCA) of foliar variables.

10.3389/fsoil.2026.1746654

TABLE 7 Analysis of variance of the $ZnSO_4$ × RFP interaction on relative uptake (foliar Cd^{2+}/soil Cd^{2+}).

Term	Sumsq	Df	Statistic	P-value
$ZnSO_4$ dose	170.9	1	11.59	0.01
Phosphoric rock dose (RFP)	33.51	1	2.27	0.18
Soil pH	1.05	1	0.07	0.8
Soil Cd^{+2} ($mg{\cdot}kg^{-1}$)	59.68	1	4.05	0.09
$ZnSO_4$ dose and Phosphoric rock dose (RFP)	188.78	1	12.81	0.01
Residuals	88.44	6		

interaction dependent on RFP level (see Tables 7, 12 for statistical inference and effect size).

3.5 Treatment comparisons derived from boxplot analyses

3.5.1 Root length

A clear separation among treatments was evidenced. Groups T2 and T3 exhibited the highest medians (≈32–40 cm) and narrow to moderately sized boxes, indicating strong performance and good consistency. In contrast, T11 and T12 showed substantially lower medians (≈7–10 cm) with small boxes, reflecting limited root development. Individual outliers (potential atypical individuals) were observed in T3 and T8, consistent with the high interplant variability noted. These patterns align with the high CV for root length (Table 4) and suggest that management factors, specifically the combinations of $ZnSO_4$ and RFP, strongly influence root development (Figure 10).

3.5.2 Root volume

The highest volumetric performance was observed in T4 (median ≈ 3–4 mL), accompanied by wide dispersion (long whiskers), indicating strong root formation potential but also considerable intra-treatment heterogeneity. Treatments T1, T2, T3, and T9 consistently showed values below 2 mL, as indicated by compact boxplots, suggesting lower root volume accumulation capacity. Overall, the mean was moderate (M = 1.91 mL; Table 4), but the variation among treatments highlights meaningful practical effects in root volume responses (Figure 11).

3.5.3 Stem diameter

Differences between treatments were more subtle (consistent with the CV ≈ 10% reported in Table 2). The best median values were observed in T6 and T8 (≈4.8–5.0 mm), followed by T4, T5, and T7, all of which showed narrow boxplots indicative of robust and homogeneous yield. The T9 group presented the lowest medians (≈3.7–4.0 mm) and greater relative dispersion. Overall, stem

TABLE 8 Slope analysis of the Zn^{2+}–Cd^{2+} foliar relationship by RFP level.

Soil cadmium ($mg{\cdot}kg^{-1}$)	Soil pH	Foliar zinc ($mg{\cdot}kg^{-1}$)	Foliar cadmium ($mg{\cdot}kg^{-1}$)	Relative uptake
1	0.84	0.49	0.96	-0.51
0.84	1	0.44	0.87	-0.6
0.49	0.44	1	0.56	0.06
0.96	0.87	0.56	1	-0.4
-0.51	-0.6	0.06	-0.4	1

TABLE 9 Global analysis of the foliar Zn^{2+}–Cd^{2+} relationship by RFP level.

Phosphoric rock (g)	$ZnSO_4$ (mg)	Treatments	Foliar cadmium ($mg{\cdot}kg^{-1}$)	Foliar zinc ($mg{\cdot}kg^{-1}$)	Soil cadmium ($mg{\cdot}kg^{-1}$)	Relative uptake
0	0	1	0.92	35.95	0.04	26.11
0	98.8	1	0.98	67.97	0.04	25.43
0	197.5	1	1.08	75.1	0.03	33.73
0	527.8	1	1.27	79.79	0.02	53.12
57.27	0	1	11.64	50.19	0.42	27.42
57.27	98.8	1	14.66	73.62	0.42	34.68
57.27	197.5	1	12.57	76.1	0.39	32.22
57.27	527.8	1	11.98	82.28	0.36	33.27
114.55	0	1	17.8	62.72	0.89	20.04
114.55	98.8	1	21.41	95.95	0.75	28.66
114.55	197.5	1	20.42	118.34	0.76	26.84
114.55	527.8	1	16.62	119.76	0.63	26.19

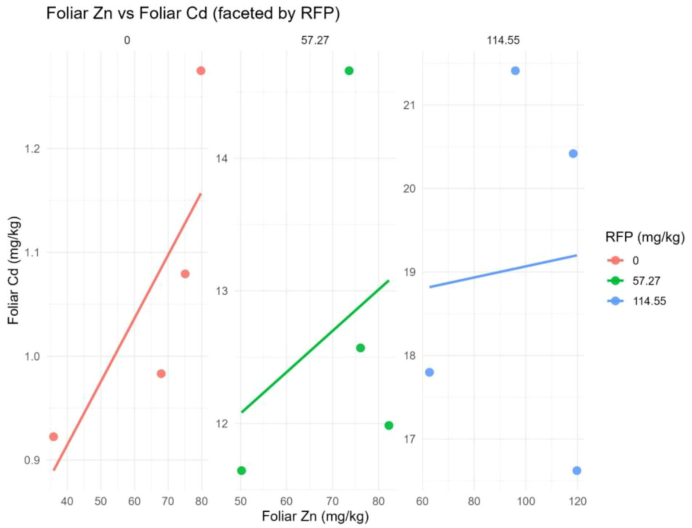

FIGURE 7
Scatter plots showing foliar Zn^{2+}–Cd^{2+} interactions across phosphate rock (RFP) levels.

diameter (mm) appears to be less sensitive to the combination of amendments than the other evaluated variables (Figure 12).

3.5.4 Number of leaves

Maximum leaf yield was observed in T6 and T8 (medians ≈ 13–14 leaves), whereas T9 and T11 showed the lowest values (≈ 7–8 leaves). T10 displayed a notably extensive interquartile range (≈ 6–15 leaves), indicating a heterogeneous response within the treatment, possibly reflecting sensitivity to micro-variations in dose or interactions with other environmental or management conditions (Figure 13).

3.5.5 Seedling height

The highest values were observed in T2, T4, and T6 (medians ≈ 32–35 cm), each showing moderate box sizes. At the lower end were T11, T12, and T9 (≈ 20–25 cm). This pattern confirms that the $ZnSO_4$ × RFP combinations that promote root development (Figures 10, 11) also lead to greater aerial height, aligning with the overall descriptive statistics (Table 4; the 95% CI of the mean height does not overlap with the lowest levels recorded in T11–T12) (Figure 14).

The boxplot results revealed that treatments with higher biometric performance (e.g., T2, T4, T6, and T8) exhibited

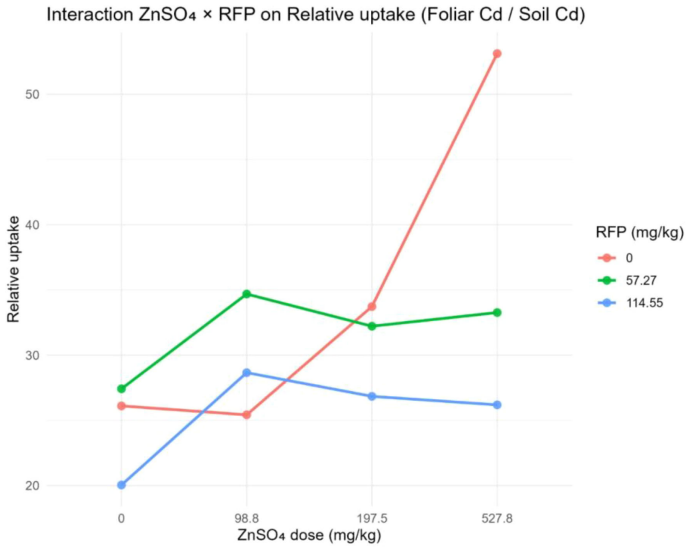

FIGURE 8
Scatter plots illustrating the $ZnSO_4$ × RFP interaction effects on the relative uptake ratio (foliar Cd^{2+}/soil Cd^{2+}).

TABLE 10 Descriptive analysis of biometric parameters in 4-month-old cocoa seedlings.

Variable	Vars	N	Mean	Sd	Median	Min	Max	Range	Skew	Kurtosis	Se
Height (cm)	1	36	27.83	4.66	27.1	19.8	36.5	16.7	-0.02	-1.23	0.78
Number of leaves	2	36	10.92	2.41	11	6	15	9	-0.29	-0.63	0.4
Stem diameter (mm)	3	36	4.38	0.44	4.5	3.47	5.17	1.7	-0.29	-1.11	0.07
Root lenght (cm)	4	36	21.35	9.79	20.6	6	42	36	0.22	-1.12	1.63
Root volume (mL)	5	36	1.91	0.88	2	1	4	3	0.7	-0.43	0.15

greater root length and volume (Figures 10, 11), as well as increased seedling height and number of leaves (Figures 13, 14). In contrast, the lowest-performing treatments (T11, T12, and T9) consistently displayed reduced values across these metrics. Given the relative stability of stem diameter (Figure 12; CV ≈ 10%), treatment effects appear to manifest primarily through longitudinal growth and root biomass, rather than stem thickening.

In terms of magnitude, the median differences between treatment extremes were significant for root length (approximately 4–5 times) and moderate for root volume (approximately 2–3 times), whereas for stem diameter, the difference was small to moderate (approximately 0.8–1.3 mm). These contrasts, together with the overall 95% CIs (Table 4), support the practical relevance of the $ZnSO_4$ × RFP intervention in mitigating Cd^{2+} impacts by enhancing root system development and, consequently, early vegetative vigour.

TABLE 11 Analysis of variance of the $ZnSO_4$ × RFP interaction on foliar Cd^{2+}.

Term	Sumsq	Df	Statistic	P-value
$ZnSO_4$ dose	6.70E-07	1	1.80E-07	1.00E+00
Phosphoric rock dose (RFP)	4.10E+00	1	1.10E+00	3.30E-01
Soil pH	9.40E+00	1	2.60E+00	1.60E-01
Soil Cd^{+2} ($mg{\cdot}kg^{-1}$)	5.60E+00	1	1.50E+00	2.60E-01
$ZnSO_4$ dose and Phosphoric rock dose (RFP)	1.20E+01	1	3.20E+00	1.20E-01
Residuals	2.20E+01	6		

3.6 Linear discriminant analysis

A multigroup LDA was conducted using biometric variables as predictors and treatment as the grouping factor. The classification performance shown in the figure corresponds to an apparent accuracy of 81% (≈29 correct classifications out of 36 observations), which is markedly higher than the accuracy expected by chance (≈8.3% with 12 groups). An approximate 95% confidence interval for accuracy ranges from 0.68 to 0.93.

Regarding the separation structure, LD1 accounted for most of the separation among treatments (horizontal distribution, as shown in Figure 15), while LD2 provided secondary differentiation (vertical distribution). In practical terms, treatments with high LD1 values (right side of the plot; e.g., T11, T8, T9) exhibit a relatively stronger biometric profile, characterized by linear combinations reflecting greater height and diameter, and, to a lesser extent, root length, compared with treatments on the negative side of LD1. Treatments with negative LD1 values (left side; e.g., T2, T3) cluster seedlings with comparatively lower

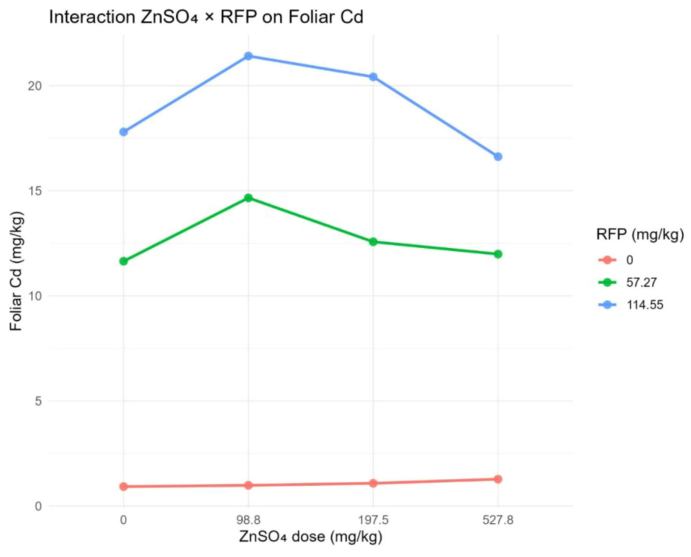

FIGURE 9
Scatter plots illustrating the $ZnSO_4$ × RFP interaction effects on foliar Cd^{2+} concentration.

10.3389/fsoil.2026.1746654

TABLE 12 Eta-squared (η^2) of the $ZnSO_4$ × RFP interaction on relative uptake (foliar Cd^{2+}/soil Cd^{2+}).

Term	Sumsq	Partial Eta2
$ZnSO_4$ dose	170.9	0.66
Phosphoric rock dose (RFP)	33.51	0.27
Soil pH	1.05	0.01
Soil Cd^{+2} ($mg{\cdot}kg^{-1}$)	59.68	0.4
$ZnSO_4$ dose and Phosphoric rock dose (RFP)	188.78	0.68
Residuals	88.44	0.5

biometric values. LD2 adds further separation for specific subsets. For example, T1 and T12 are distinguished from others with similar LD1 values but different LD2 positions, suggesting contrasts along an orthogonal trait combination (e.g., root volume and leaf number versus height/diameter), which helps explain certain overlaps and classification errors. The central cluster, where several intermediate treatments (e.g., T4–T7) overlap, accounts for the misclassification fractions contributing to the overall 81% accuracy. From an experimental interpretation perspective, these intermediate treatments share similar biometric phenotypes, consistent with $ZnSO_4$ × RFP combinations that do not generate strong contrasts in seedling growth.

Within the framework of the research project "Antagonistic interaction between zinc sulphate and cadmium in cocoa seedlings (*Theobroma cacao* var. CCN-51) under phosphate rock application", the observed separation indicates that biometric responses integrate the Zn^{2+}–Cd^{2+} interaction signal as modulated by RFP. Treatments combining conditions that favour Zn^{2+}↔Cd^{2+} antagonism tend to cluster at one extreme of LD1 (reflecting superior biometric performance), whereas less favourable combinations appear at the opposite extreme (reflecting poorer performance). The pattern of partial overlap suggests that, although the overall signal is strong, there is intragroup heterogeneity (e.g., variation among pots or individual seedlings) that should be more tightly controlled in future experimental designs.

3.7 Ranking of relative cadmium uptake (foliar Cd/soil Cd)

In Figure 15 and Table 2, relative uptake (foliar Cd^{2+}/soil Cd^{2+}; lower values indicate better performance) varied widely among treatments (range = 33.08; maximum in T4 = 53.12; minimum in T9 = 20.04). The relative difference between the worst and best treatments was 62.3% = 1 − (20.04/53.12), indicating a substantial potential for reducing Cd^{2+} transfer to leaf tissue. Ranked from best to worst (lowest to highest relative uptake), the five treatments with the lowest values were: T9 (20.04), T2 (25.43), T1 (26.11), T12 (26.19), and T11 (26.84), as shown in Table 2. At the opposite end of the distribution, the treatments with the highest relative uptake were T4 (53.12), T6 (34.68), T3 (33.73), and T8 (33.27).

The colour of the bars encodes the dose of phosphate rock (RFP): 0 $mg{\cdot}kg^{-1}$ (red), 57.27 $mg{\cdot}kg^{-1}$ (green), and 114.55 $mg{\cdot}kg^{-1}$ (blue). Based on the values in Table 4, the averages within each RFP level were as follows: RFP = 114.55 $mg{\cdot}kg^{-1}$: ≈ 25.43 (T9, T10, T11, T12); RFP = 57.27 $mg{\cdot}kg^{-1}$: ≈ 31.90 (T5, T6, T7, T8); RFP = 0 $mg{\cdot}kg^{-1}$: ≈ 34.60 (T1, T2, T3, T4). Thus, the highest RFP dose (114.55 $mg{\cdot}kg^{-1}$) was associated with an average reduction of approximately 26.5% in relative Cd uptake compared with the 0 $mg{\cdot}kg^{-1}$ treatments (mean difference = 34.60 − 25.43 = 9.17 units). Moreover, intragroup variability was substantially greater at RFP = 0 $mg{\cdot}kg^{-1}$ (range ≈ 27.69) than at RFP = 57.27 $mg{\cdot}kg^{-1}$ (≈ 7.26) or RFP = 114.55 $mg{\cdot}kg^{-1}$ (≈ 8.62), suggesting more stable control of Cd^{2+} transfer when the phosphorite dose is increased.

The ranking pattern supports the attenuation of foliar Cd^{2+} uptake under management combinations that incorporate higher RFP doses (blue bars in Figure 16), consistent with the antagonism hypothesis (i.e., reduced Cd^{2+} bioavailability through phosphate complexation and/or fixation, and/or synergistic interactions with $ZnSO_4$). In practical terms, T9 emerges as the most effective treatment (20.04), whereas

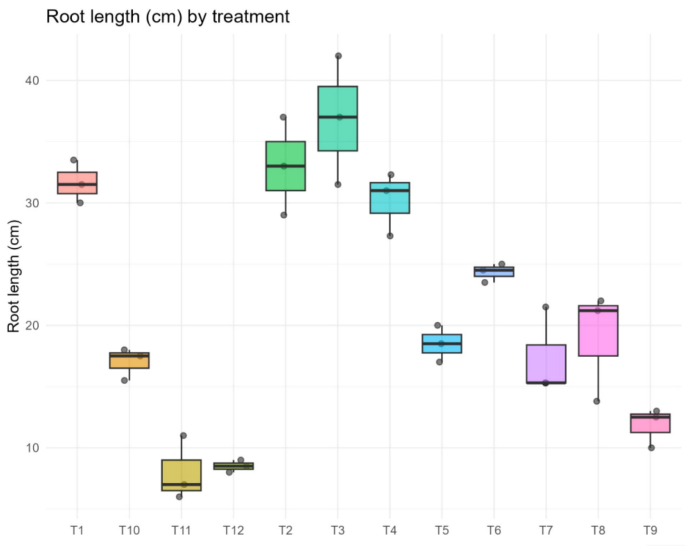

FIGURE 10
Boxplots showing the distribution of root length across treatments.

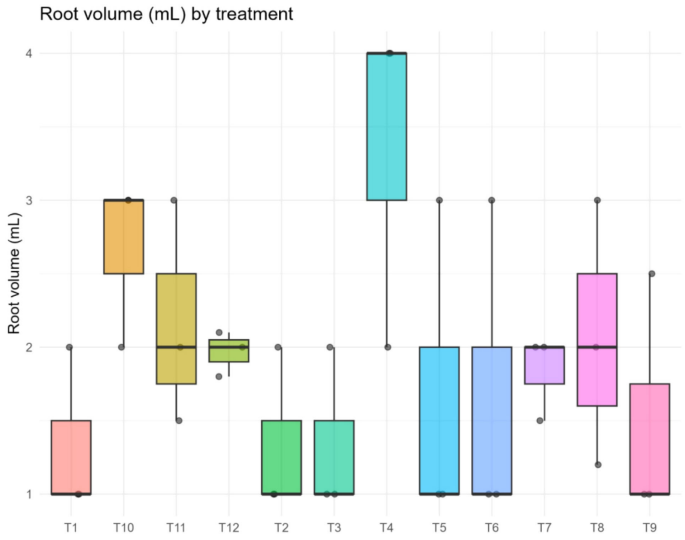

FIGURE 11
Boxplots showing the distribution of root volume across treatments.

T4 represents the least favourable scenario (53.12). Overall, the data presented in Figure 16 and Table 3 indicate that increasing RFP, together with selecting appropriate $ZnSO_4$ combinations (Figures 7–9), consistently reduces the foliar Cd^{2+}/soil Cd^{2+} ratio while also decreasing variability. This trend is both statistically and agronomically significant for minimizing Cd^{2+} accumulation in the leaf tissue of cocoa seedlings.

4 Discussions

At the biometric level, the median values for seedling height (≈30–35 cm) and stem diameter (≈4.5–5.0 mm) indicate uniform vigor with moderate dispersion (coefficient of variation ≈10–20%). In contrast, root volume exhibits greater asymmetry and much higher dispersion (high CV), a pattern frequently observed in seedlings due to the inherent plasticity of root development (24, 25). In the soil, pH values fall within the acidic to subacidic range, which is characteristic of tropical cocoa production systems and corresponds to conditions that enhance Cd^{2+} mobility (26, 27). In leaf tissue, the marked variability in Zn^{2+}, P_2O_5, and Na^+ concentrations reflects differential plant responses to $ZnSO_4$ and phosphate amendments, key factors known to modulate Cd^{2+} uptake dynamics (28, 29).

High correlations were observed in the soil between P_2O_5 and Cd^{2+} ($r \approx 0.93$), exchangeable K^+ ($r \approx 0.97$), and exchangeable Na^+ ($r \approx 0.95$), as well as between pH and P_2O_5 ($r \approx 0.73$). These results are consistent with the co-mobilization of Cd^{2+} alongside available phosphates in acidic soils, even though phosphate rock generally tends to immobilize Cd^{2+} through precipitation as Cd-phosphates

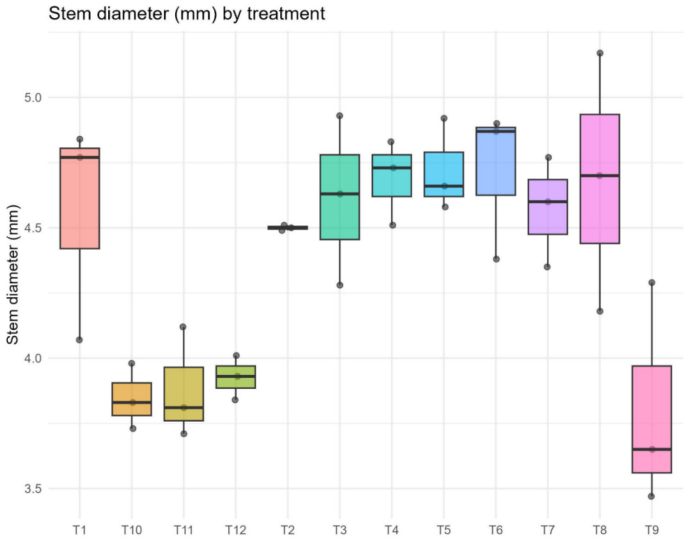

FIGURE 12
Boxplots showing the distribution of seedling stem diameter across treatments.

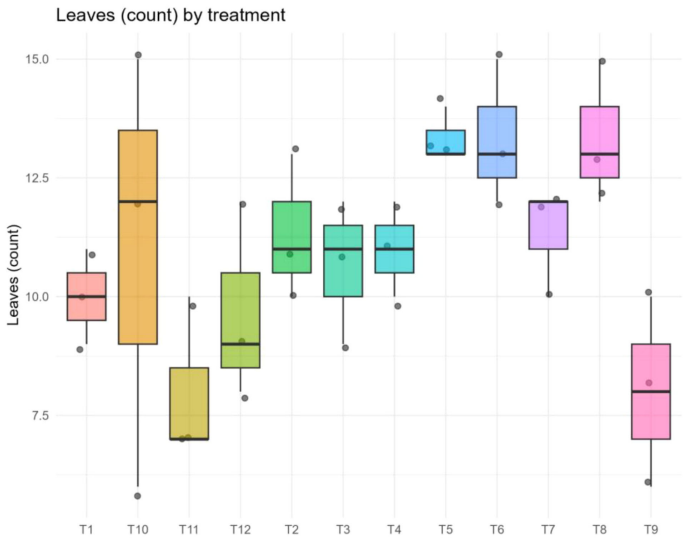

FIGURE 13
Boxplots showing the distribution of the number of leaves per seedling across treatments.

when pH and Ca-phosphate concentrations increase (28, 30, 31). The magnitude of the Zn–Cd association ($r \approx 0.73$) suggests the presence of shared edaphic gradients; however, at the physiological level, Zn^{2+} competes with Cd^{2+} at the root interface, potentially reducing Cd^{2+} translocation despite their co-occurrence in the soil matrix (28, 32).

Leaf analysis revealed a strong correlation between P_2O_5 and foliar Cd^{2+} ($r \approx 0.88$), as well as substantial correlations for P_2O_5–Na^+ ($r \approx 0.77$) and K_2O–Zn^{2+} ($r \approx 0.72$). The Zn^{2+}–Cd^{2+} association was moderately positive ($r \approx 0.59$). Two complementary mechanisms may explain these patterns: (i) competition between Zn^{2+} and Cd^{2+} for ZIP/NRAMP transporters, which can reduce Cd^{2+} uptake in the presence of Zn^{2+}, although it does not necessarily eliminate covariation when both elements respond to a shared absorption gradient (29, 33); and (ii) the influence of phosphorus on Cd^{2+} speciation and on the ionic balance of cations such as Na^+ and K^+ in leaf tissue (34, 35).

In the biometric analysis of 4-month-old cocoa seedlings, a strong correlation between seedling height and root length ($r = 0.88$; $n = 36$), and a moderate correlation between seedling height and stem diameter ($r \approx 0.58$) was observed. Root volume showed only weak associations with the other variables ($|r| < 0.10$). These relationships suggest that aerial and root development covary strongly, whereas root volume, being more sensitive to micro-heterogeneity in the substrate, does not scale linearly with root length (24).

The separation of treatments along Dim1 is consistent with previously reported differences in morphological performance (36). This orientation indicates that high K^+ and Zn^{2+} availability is associated with leaf nutrient profiles that differ from those characterized by elevated P_2O_5 and Cd^{2+}, a pattern consistent

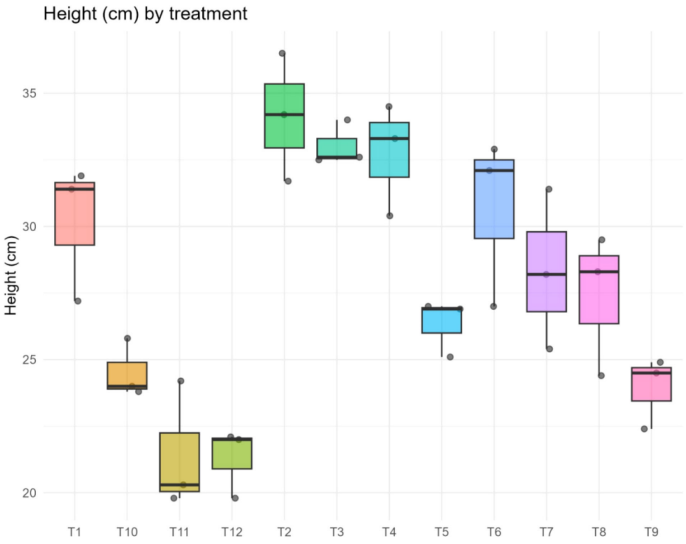

FIGURE 14
Boxplots showing the distribution of seedling height across treatments.

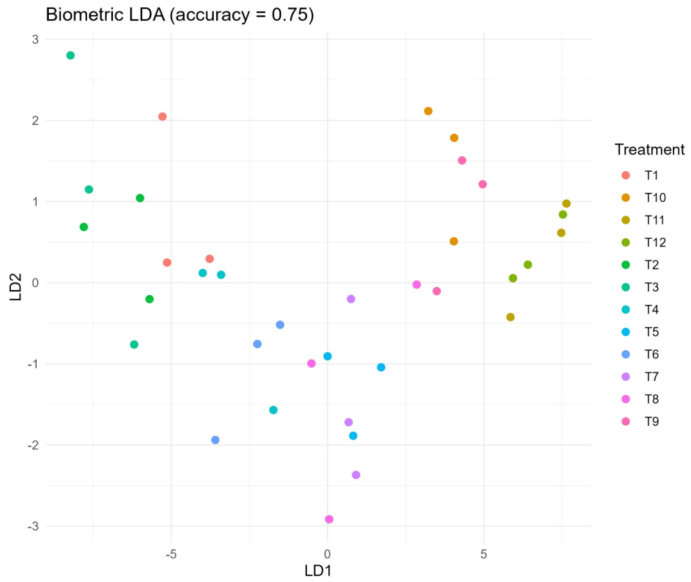

FIGURE 15
Linear Discriminant Analysis (LDA) showing the multivariate separation of 4-month-old cocoa seedling biometric traits across treatments.

with functional antagonism (29) and with cation-balance effects (37). This pattern is characteristic of acidic soils, in which available P, the exchange complex (particularly K^+), and trace metals (Cd^{2+}, Zn^{2+}) follow shared availability gradients (27, 38).

Regarding the interaction between foliar Zn^{2+} and foliar Cd^{2+} across RFP levels, the highest RFP dose (114.55 mg·kg^{-1}) was associated with greater absolute foliar Cd^{2+} concentrations compared with the lower RFP treatments. This pattern suggests that, although foliar Zn^{2+} shows a modest covariation with foliar Cd^{2+}, increasing phosphate application shifts Cd^{2+} concentrations, consistent with changes in Cd^{2+} speciation and solubility driven by phosphate chemistry and pH effects (31, 35). Accordingly, the reduced slope observed at high RFP levels indicates intensified Zn^{2+}–Cd^{2+} competition during transport and uptake processes (29, 33). In the $ZnSO_4$ × RFP interaction for relative uptake (foliar Cd^{2+}/soil Cd^{2+}), relative uptake increased with increasing $ZnSO_4$ doses; however, at RFP levels of 57.27 and 114.55 mg·kg^{-1}, this response became attenuated or even reversed. This behavior is consistent with the concept that Zn^{2+} may enhance Cd^{2+} mobility or co-induce uptake in acidic soils only under specific ionic-balance conditions. When RFP is co-applied, Cd^{2+} is progressively immobilized through the formation of Cd–phosphate precipitates, while Zn^{2+} increasingly competes for shared transport pathways, thereby reducing the foliar Cd^{2+}/soil Cd^{2+} ratio (28, 30, 32, 34).

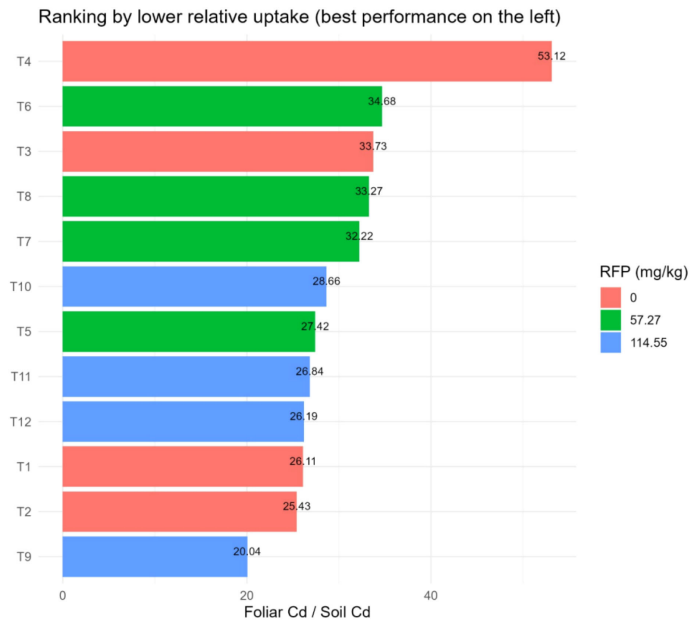

FIGURE 16
Ranking of treatments based on relative cadmium uptake (foliar Cd^{2+}/soil Cd^{2+} ratio). Lower values indicate better Cd^{2+} mitigation efficiency.

FIGURE 17
Morphological differences among root, stem, and leaf tissues of cocoa seedlings under treatments T1, T2, T3, and T4.

FIGURE 19
Morphological differences among root, stem, and leaf tissues of cocoa seedlings under treatments T9, T10, T7, and T11.

Treatments T2–T4–T6–T8 exhibited higher medians for seedling height, stem diameter, and root length, with T4 standing out for root volume (Figure 17). The dispersion among treatments suggests a combined effect of $ZnSO_4$ and RFP, consistent with the separation observed in the PCA-Seedling (Figure 18). The best biometric performance generally coincides with lower relative uptake, except under high RFP and $ZnSO_4$ conditions, where trade-offs between growth and Cd^{2+} mitigation may occur (36, 39).

The biometric LDA achieved an accuracy of approximately 0.81, indicating good separability among treatments based on morphological traits (height, diameter, root length, and number of leaves) (Figure 19). Given n = 36 and multiple groups, this level of accuracy is considered high for exploratory classification purposes (40, 41). The discriminant structure aligns with the PCA-Seedling axes, confirming consistency between both multivariate approaches (37).

The ranking (lower foliar Cd^{2+}/soil Cd^{2+} = better) positions T9, T2, T1, T12, and T11 as the top five treatments (≈20–27), whereas T4 ranks last (≈53). Notably, the best-performing treatments include both high RFP (114.55 $mg{\cdot}kg^{-1}$; T9) and no RFP (0 $mg{\cdot}kg^{-1}$; T1–T2), suggesting two distinct pathways for reducing uptake: (i) soil immobilization through RFP application (28, 30), and (ii) physiological antagonism by Zn^{2+} competition in the absence of RFP, when soil Cd^{2+} availability is relatively low (29, 32). Conversely, unfavourable combinations (e.g., T4) may reflect locally low pH and high mobile phosphorus conditions, which enhance Cd^{2+} transfer to plants (27, 31).

Treatment T4, which received 527.8 mg of zinc sulfate, exhibited the highest Cd uptake, suggesting that the application of Zn-containing fertilizers may reduce Cd accumulation in plant tissues (42). The experimental substrate consisted of natural agricultural soil collected from a cocoa plantation within the study area, representative of regional soil conditions (Figure 20). It was physically and chemically characterized prior to its use in the experiment. Evaluation of the heavy metal (HM) translocation factor (such as Cd), bioaccumulation factor, and bioconcentration factor, particularly in treatments amended with phosphate rock, highlighted the key role of *Serratia plymuthica* in limiting the mobility of toxic heavy metals such as Cd and preventing their translocation to aerial plant tissues (43, 44).

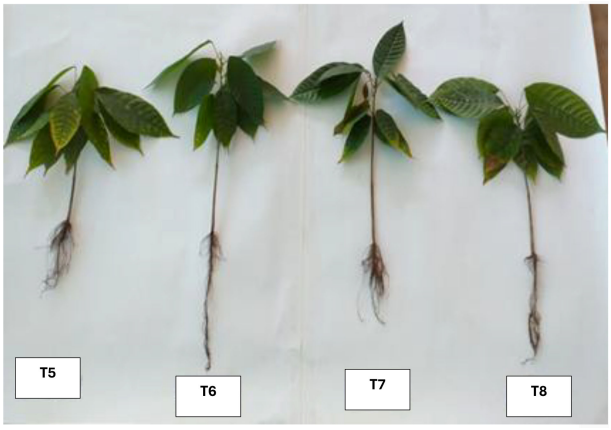

FIGURE 18
Morphological differences among root, stem, and leaf tissues of cocoa seedlings under treatments T5, T6, T7, and T8.

FIGURE 20
Morphological differences among root, stem, and leaf tissues of cocoa seedlings under three replicates of treatment T12.

5 Conclusions

Zn^{2+}–RFP conditions Cd^{2+} antagonism. The relationship between Zn^{2+} and Cd^{2+} in leaf tissue exhibited antagonistic patterns when zinc sulphate ($ZnSO_4$) was co-applied with phosphate rock (RFP). In the absence of RFP, the relative uptake (foliar Cd^{2+}/soil Cd^{2+}) tended to increase with increasing $ZnSO_4$ doses. In contrast, at medium to high RFP levels, the slope attenuated or even reversed, indicating modulation of Zn^{2+}–Cd^{2+} interactions by phosphate availability.

Soil phosphorus acted as a major modulator. Correlation matrices and soil PCA revealed a P–(Cd^{2+}, Zn^{2+})–K^+ gradient opposite to that of pH/Na^+. The high correlation coefficients (r) observed in the soil indicate that phosphorus availability and pH explain a significant portion of the covariation between Cd^{2+} and Zn^{2+} in the soil matrix, and consequently, their transfer to plants.

The foliar PCA (F5) showed that K_2O_5 and Zn^{2+} accounted for most of the variance along Dim1 (67.6%), whereas P_2O_5 and Cd^{2+} projected in the opposite direction. This pattern supports a cationic balance conducive to Zn^{2+}–Cd^{2+} functional antagonism when the system is enriched with phosphate.

Plant growth was structured along two axes. The seedling PCA revealed a morpho-structural vigour axis (seedling height, root length, and stem diameter; Dim1 = 50.8%) and a root mass/volume axis (Dim2 = 20.8%). These components explain the separation between treatments observed in the boxplots.

Consistent biometric associations were reported across the trait level. Seedling height showed a strong correlation with root length ($r \approx 0.88$; $n = 36$) and a moderate correlation with stem diameter ($r \approx 0.58$), confirming that aerial and root vigour covaried across the evaluated treatments.

In leaves, P_2O_5–Cd^{2+} showed a strong correlation ($r \approx 0.88$) and Zn^{2+}–Cd^{2+} a moderate one ($r \approx 0.59$). The first suggests that variations in available phosphorus may co-modulate Cd^{2+} accumulation in leaf tissue, while the second indicates that, although Zn^{2+} and Cd^{2+} covary along shared uptake gradients, the net effect of Zn^{2+} on Cd^{2+} is contingent on the phosphate context.

The biometric LDA achieved an accuracy of ≈0.81, demonstrating clear multivariate differentiation among treatments based on height, diameter, number of leaves, and root length. This classification structure is consistent with the axes identified in the seedling PCA, reinforcing the robustness of the morphological pattern.

The morphological performance by treatment, as depicted in the boxplots, revealed higher growth medians in T2, T3, T4, T6, and T8, depending on the variable assessed. Overall, combinations involving RFP and moderate $ZnSO_4$ doses exhibited superior morphological responses.

The relative uptake ranking identified T9, T2, T1, T12, and T11 as the top five treatments (lowest foliar Cd^{2+}/soil Cd^{2+} ≈20–27), whereas T4 showed the lowest performance (≈53). These results suggest two effective mechanisms for reducing Cd^{2+} transfer: (a) soil immobilization through high RFP application (e.g., T9), and (b) physiological Zn^{2+}–Cd^{2+} competition under conditions of low soil Cd^{2+} availability (e.g., T2).

Therefore, based on the conducted analyses, it can be concluded that the convergence between the correlation, PCA, interaction, and LDA results supports the existence of Zn^{2+}–Cd^{2+} antagonism; however, its expression is modulated by pH and, most importantly, by the availability of phosphorus derived from RFP.

Data availability statement

The original contributions presented in the study are included in the article/supplementary material. Further inquiries can be directed to the corresponding author.

Author contributions

HD: Visualization, Investigation, Writing – original draft, Conceptualization, Writing – review & editing. MM: Methodology, Software, Writing – original draft. GV: Writing – original draft, Data curation, Resources. JC: Writing – review & editing, Validation. HH: Supervision, Writing – review & editing. MS: Formal analysis, Writing – review & editing. RS: Project administration, Writing – review & editing, Funding acquisition. BM: Writing – original draft.

Funding

The author(s) declared that financial support was received for this work and/or its publication. The research was funded by the Instituto Nacional de Innovación Agraria, within the framework of the project: Mejoramiento de los servicios de investigación y transferencia tecnológica en el manejo y recuperación de suelos agrícolas degradados y aguas para riego en la pequeña y mediana agricultura en los departamentos de Lima, Áncash, San Martín, Cajamarca, Lambayeque, Junín, Ayacucho, Arequipa, Puno y Puno y Ucayali" CUI 2487112.

Conflict of interest

The author(s) declared that this work was conducted in the absence of any commercial or financial relationships that could be construed as a potential conflict of interest.

Generative AI statement

The author(s) declared that generative AI was not used in the creation of this manuscript.

Any alternative text (alt text) provided alongside figures in this article has been generated by Frontiers with the support of artificial intelligence and reasonable efforts have been made to ensure accuracy, including review by the authors wherever possible. If you identify any issues, please contact us.

Publisher's note

References

1. ICCO. Quarterly Bulletin of Cocoa Statistics. International Cocoa Organization (2024). Available online at: https://www.icco.org/november-2024-quarterly-bulletin-of-cocoa-statistics/ (Accessed November 6, 2025).

2. Charry A, Perea C, Ramírez K, Zambrano G, Yovera F, Santos A, et al. The bittersweet economics of different cacao production systems. *Agric Syst*. (2025). Available online at: https://edepot.wur.nl/683478 (Accessed December 1, 2025).

3. European Commission. Commission Regulation (EU) 2023/915 on maximum levels for certain contaminants in food. EUR-Lex (2023). Available online at: https://eur-lex.europa.eu/eli/reg/2023/915/oj/eng (Accessed November 8, 2025).

4. MIDAGRI. Observatorio de Commodities – Cacao (N.° 02/2024). Perú: Ministerio de Desarrollo Agrario y Riego (2024). Available online at: https://repositorio.midagri.gob.pe/bitstream/20.500.13036/1960/1/Comodities-cacao-n-02-2024.pdf (Accessed November 7, 2025).

5. MIDAGRI-DEE. Dinámica productiva de café, cacao y palma aceitera en el departamento de Loreto. Dirección de Estudios Económicos – MIDAGRI (2025). Available online at: https://repositorio.midagri.gob.pe/bitstream/20.500.13036/1977/1/Loreto-dinamica-productiva.pdf (Accessed December 7, 2025).

6. Thomas E, Atkinson R, Zavaleta D, Rodríguez C, Lastra S, Yovera F, et al. The distribution of cadmium in soil and cacao beans in Peru. *Sci Total Environ*. (2023) 881:163372. doi: 10.1016/j.scitotenv.2023.163372

7. CATIE. Cadena de valor del cacao en San Martín (Perú). Repositorio CATIE (2023). Available online at: https://repositorio.catie.ac.cr/bitstream/handle/11554/4943/BCO23089240e.pdf?isAllowed=y&sequence=1 (Accessed November 11, 2025).

8. Bravo D, Araujo-Carrillo G, Carvalho F, Chaali N, León-Moreno C, Quiroga-Mateus R, et al. First national mapping of cadmium in cacao beans in Colombia. *Sci Total Environ*. (2024) 954:176398. Available online at: https://www.sciencedirect.com/science/article/abs/pii/S0048969724065549 (Accessed November 11, 2025).

9. Vallejos-Torres G, Chuchon-Remon RJ, Gaona-Jimenez N, Cruz-Luis J, Solórzano-Acosta R. Cadmium distribution and soil properties across soil orders under cacao (*Theobroma cacao* L.) cultivation in the Peruvian Amazon. *Front Soil Sci*. (2025) 5:1686799. doi: 10.3389/fsoil.2025.1686799

10. Luis-Alaya B, Toro M, Calsina R, Ogata-Gutiérrez K, Gil-Polo A, Ormeño-Orrillo E, et al. Evaluation of the Presence of Arbuscular Mycorrhizae and cadmium content in the plants and soils of cocoa plantations in San Martin, Peru. *Diversity*. (2023) 15:246. doi: 10.3390/d15020246

11. Vallejos-Torres G, Gaona-Jimenez N, Alva Arevalo A, Paredes C, Lozano A, Saavedra-Ramírez J, et al. Cadmium uptake and mycorrhization by cacao clones in agroforestry and monoculture systems of Peruvian Amazon. *Bioagro*. (2023) 35:237–46. doi: 10.51372/bioagro353.7

12. SENAMHI. Aviso metereológico del Perú (2025). Available online at: https://www.senamhi.gob.pe/?p=aviso-meteorologico-vigente&a=2025&b=20222&c=00&d=SENA (Accessed December 1, 2025).

13. R Core Team. R: A language and environment for statistical computing. R Foundation (2025). Available online at: https://www.r-project.org/r-project.org. (Accessed November 9, 2025).

14. Posit team. RStudio: Integrated Development Environment for R. Posit Software, PBC (2025). Available online at: https://posit.co/downloads/Posit (Accessed December 6, 2025).

15. Wickham H, Çetinkaya-Rundel M, Grolemund G. R for Data Science (2023). Available online at: https://r4ds.hadley.nz/r4ds.hadley.nz (Accessed December 7, 2025).

16. Makowski D, Lüdecke D, Patil I, Thériault R, Ben-Shachar M, Wiernik B. report: Automated Reporting of Results and Statistical Models (v0.6.1) [R package]. CRAN (2025). Available online at: https://cran.r-project.org/package=reportcran.r-project.org (Accessed November 13, 2025).

17. Wei T, Simko V. corrplot: Visualization of a Correlation Matrix (v0.95) [R package]. CRAN (2024). Available online at: https://cran.r-project.org/package=corrplotcran.r-project.org (Accessed December 14, 2025).

18. James G, Witten D, Hastie T, Tibshirani R. *An introduction to statistical learning. 2nd ed*. Springer (2021). doi: 10.1007/978-1-0716-1418-1

19. Kassambara A, Mundt F. factoextra: Extract and visualize the results of multivariate data analyses (v1.0.7) [R package]. CRAN (2025). Available online at: https://cran.r-project.org/package=factoextracran.r-project.org (Accessed December 11, 2025).

20. Fox J. car: Companion to Applied Regression (v3.1-3) [R package]. CRAN (2024). Available online at: https://cran.r-project.org/package=carcran.r-project.org (Accessed December 9, 2025).

21. Hayes AF. Introduction to mediation, moderation, and conditional process analysis. *3rd ed*. Guilford Press (2022). Available online at: https://www.guilford.com/books/Introduction-to-Mediation-Moderation-and-Conditional-Process-Analysis/Andrew-Hayes/9781462549030 (Accessed December 8, 2025).

22. Wickham H, Navarro D, Pedersen TL. ggplot2: Elegant graphics for data analysis (2024). Available online at: https://ggplot2-book.org/ggplot2-book.org (Accessed November 29, 2025).

23. Jia S, Zhang Y, Liu Y, Wang S. Phosphorus alleviates cadmium damage by reducing Cd uptake in soybean. *Agronomy*. (2025) 15:637. Available online at: https://www.mdpi.com/2073-4395/15/3/637. (Accessed December 4, 2025).

24. Jin R, Li Z, Wang X, Liu F, Kong F, Liu Q, et al. Morphological trait diversity in T. cacao using PCA. *Agronomy*. (2023) 13:462. doi: 10.3390/agronomy13020462

25. Mendoza-Arenas JJ, et al. Nutritional status and yield relationships in cocoa …. *Agronomy*. (2021) 11:1965. doi: 10.3390/agronomy11101965

26. Arévalo-Gardini E, et al. Factors affecting cadmium accumulation in cacao …. *Agronomy*. (2021) 11:1841. doi: 10.3390/agronomy11091841

27. Wu P, et al. Effects of soil pH management on Cd availability. *Sci Total Environ*. (2023) 857:159605. doi: 10.1016/j.scitotenv.2022.159605

28. Wang S, et al. Interactions between zinc and cadmium in soils/plants. *J Hazardous Mater*. (2022) 427:127890. doi: 10.1016/j.jhazmat.2021.127890

29. Xue T, et al. Zinc ameliorates cadmium toxicity: Mechanisms. *Front Physiol*. (2023) 14:1195801. doi: 10.3389/fphys.2023.1195801

30. Qin X, et al. Apatite-based amendments for heavy-metal soils. *JECE*. (2024) 12:111077. doi: 10.1016/j.jece.2024.111077

31. Medeiros AM, et al. Phosphorus amendments modulate cadmium speciation …. *Geoderma*. (2020) 370:114339. doi: 10.1016/j.geoderma.2020.114339

32. Montalvo D, et al. Competitive interactions of Cd and Zn at the soil–root interface. *Plant Soil*. (2020) 448:165–89. doi: 10.1007/s11104-019-04114-7

33. Cao Q, et al. Foliar zinc application reduces cadmium accumulation …. *Environ pollut*. (2024) 335:122906. doi: 10.1016/j.envpol.2023.122906

34. Liu R, et al. Mechanisms of cadmium immobilization by phosphate amendments. *J Hazardous Mater*. (2021) 403:123676. doi: 10.1016/j.jhazmat.2020.123676

35. Bolan NS, et al. Liming and phosphate amendments …. *Environ pollut*. (2022) 300:118932. doi: 10.1016/j.envpol.2022.118932

36. Shah AA, Bibi F, Hussain I, Yasin NA, Akram W, Tahir MS, et al. Variability of nutrients in cacao clones via PCA. *Plants*. (2020) 9:1512. doi: 10.3390/plants9111512

37. Kuhn M, Johnson K. *Feature Engineering and Selection (caps. PCA/LDA)*. CRC (2020). doi: 10.1201/9781315108230

38. Joshi-Saha A, Sethy SK, Misra G, Dixit GP, Srivastava AK, Sarker A. Long-term field performance of hydroxyapatite. *Field Crops Res*. (2022) 279:108467. doi: 10.1016/j.fcr.2022.108467

39. Pujara Y, Govani J, Patel HT, Pathak P, Mashru D, Ganesh PS. Soil and leaf factors controlling cadmium in Ecuadorian cacao. *Environ Adv*. (2024) 15:100364. doi: 10.1016/j.envadv.2023.100364

40. Rohlf FJ, Corti M. Use of discriminant analysis revisited. *Syst Biol*. (2020) 69:1304–13. doi: 10.1093/sysbio/syaa020

41. Duan M, Zhang X. Using remote sensing to identify soil types based on multiscale image texture features. *Comput Electron Agric*. (2021) 187:106272. doi: 10.1016/j.compag.2021.106272

42. Gray CW, Wise BE. Can the application of zinc decrease cadmium concentrations in spinach in a zinc sufficient soil? *New Z J Crop Hortic Sci*. (2020) 48:117–29. doi: 10.1080/01140671.2020.1745247

43. Sai A, Ben Younes S, Ellafi A, Moula A, Sánchez-Yañez JM, Borgi MA, et al. Exploration and impact of Metlaoui-Gafsa phosphate rock amendment: the role of Serratia plymuthica BMA1 in phosphate solubilization, heavy metal rhizoaccumulation, and enhanced nutrition in Vicia faba L. *Environ Sci pollut Res*. (2024) 31:67007–23. doi: 10.1007/s11356-024-35604-9

44. Borgi MA, Saidi I, Moula A, Rhimi S, Rhimi M. The Attractive Serratia plymuthica BMA1 Strain With High Rock Phosphate-Solubilizing Activity and Its Effect on the Growth and Phosphorus Uptake by Vicia faba L. *Plants Geomicrobiol J*. (2020) 37:437–45. doi: 10.1080/01490451.2020.1716892